13th International Symposium on Particle Image Velocimetry – ISPIV 2019
Munich, Germany, July 22-24, 2019

Experimental Investigation on Fluid Mechanics of Different Micro Heat Transfer Devices

M. Spizzichino[1]*, G. Sinibaldi[1], G.P. Romano[1]
[1] Sapienza University, Dept. Mechanical and Aerospace Engineering, Roma, Italy
*michela.spizzichino@uniroma1.it

Abstract

The future technological horizons for engineering applications (Automotive, Energy, Bio-engineering) will require the use of limited size heat exchangers with high heat exchange efficiency. In the present work, the flow field in micro channels of different geometries is investigated experimentally using μPIV (micro Particle Image Velocimetry) and thermal measurements. The Reynolds number in the channels is changed as also the wall temperature, in order to investigate and improve the thermal exchange efficiency at different flow rates, temperatures and geometrical configurations. The main result of this investigation is that the standard serpentine micro cell attains the highest heat exchange efficiency regardless of flow regime, getting high Nusselt numbers combined with low pressure losses, due to quite high local velocities and few recirculation regions.

1 Introduction and Problem Statement

The use of high efficiency heat exchangers is the basis of several technological developments required in different engineering applications, e.g. automotive, energy and bioengineering (Eshani et al. (2005)). Since the heat transfer coefficient is inversely proportional to the characteristic dimension of the system as shown by Massoud (2005), a valid solution to optimize the cooling process is to use a system of multiple micro heat exchangers instead of a single macro counterpart. Until now, the main features usually investigated to enhance the heat transfer efficiency of micro-devices are related to the materials of the microchannel, the channel geometry, the cooling fluid and the flow regime (Kandlikar et al. (2012), Kandlikar et al. (2013)). To this aim, the heat transfer performances of a small-device are commonly assessed by the ratio between the heat transfer rate, usually expressed in terms of the average Nusselt number, based on the difference between inlet and outlet temperature of the working fluid, and the pressure losses induced by the geometry, which can be directly measured or analytically determined on the base of boundary conditions as described by Al-Neama et al. (2017) (in section 3 exact definitions are given).

From the 90s up to today, several studies have been carried out to optimize the channel geometry and the flow regime (Asako et al. (1988), Gaiser et al. (1989), Herman et al. (1991), Fehle et al. (1995)). In particular, heat exchangers with channels having a serpentine shape have received considerable attention given the high heat transfer properties and the compactness requirement typical of such micro-devices. The first work introducing a periodical deflection of the flow in a meandering arrangement of a straight channel is due to Asako et al. (1988). The use of such a meandering micro-channel leads to an increase of heat transfer in comparison to the straight channel of 77% for a Reynolds number (Re) around 1000. This is related to enhancements of local turbulence levels in meanders, at the cost of a large increase in pressure drop, i.e. around 95%. From this first study, it was clear how transition to turbulent regime increases the thermal diffusion from a molecular to a macroscopic level. As a consequence, other studies have increasingly focused on the research of new geometrical solutions to promote turbulence motions within straight channels. The main proposals concern corrugated walls (Gaiser et al. (1989)), channel side grooving (Herman et al. (1991)) and cylindrical ribs fixed in a staggered or in line arrangements (Fehle et al. (1995)). However, all these solutions, while promoting large deflections and velocity changes in the fluid flow, were characterized by moderate increase in the average Nusselt number compared with a large increase in pressure drop. Then, starting from 2000s,

geometries have been designed to obtain high increases in Nusselt number by keeping low pressure losses. Despite the good thermal properties attainable by the U-shaped serpentine micro-channels, Al-Neama et al. (2017) proposed an experimental and numerical work showing how this configuration, as also more complicated options, are affected by a high temperature gradient, between the inlet and the outlet of the fluid flow, leading to a consequent large inhomogeneity in the heat exchange process. Sui et al. (2011), already in 2011, pointed out this problem and proposed a solution through an experimental investigation of three sinusoidal micro-channels with rectangular cross sections and different wavy amplitudes. More in detail, their experimental study revealed that under laminar flow regime (300<Re<800), in a straight channel or section, as for example in the standard serpentine microchannel, the heat transfer performances deteriorate along the flow direction because the flow becomes more regular and the boundary layers thicken, so that temperature gradients become increasingly small. However, by inserting periodic curvilinear sections, the generated secondary flows enhance fluid mixing, thus decreasing the temperature gradient between inlet and outlet. Based on these preliminary results, great interest has been given to the study of a wavy-sinusoidal configuration and to the evaluation of solutions to increase its heat exchange properties. In particular, Lin et al. (2017) improved the heat transfer properties through the design of a wavy microchannel with changing wavelength and amplitude along the flow direction. From the comparison between the new and the standard wavy-sinusoidal configuration, it is possible to notice a considerable increase in heat transfer and a lower inhomogeneity in the thermal field, due to the formation of vortices of different size in the channel cross sections. However, even with such a considerable improvement of the wavy-sinusoidal configuration performances, i.e. efficiency around 52% at Re = 800 (Sui et al. (2011)), the efficiency is not yet comparable with that of the serpentine configuration, around 71% at the same Reynolds number (Al-Neama et al. (2017)). From the above mentioned literature, it is evident the importance of experimental investigations on new geometrical solutions, combining the simple geometry and low pressure losses of the U-shaped serpentine with the heat transfer improvements of the wavy-sinusoidal.

Hence, in the present work, the thermo-hydrodynamic behaviours of two square cross-section (1 x 1 mm^2) serpentine micro-channels are investigated, i.e. a conventional serpentine and a new wavy-sinusoidal serpentine. Results are evaluated in terms of efficiency of the cell and compared with a classical straight parallel channel micro cell, to be considered as reference. In addition, to test the heat transfer properties and the detailed fluid flow behaviour, this research was extended from typical range of Reynolds number in the laminar regime, from 50 to 1500, up to Reynolds number of 4000, i.e. in the turbulent regime. The aim of the present work is to explore and compare the thermal performances of conventional and novel wavy serpentine micro-channels. The heat exchange efficiencies are evaluated by means of the Nusselt-Reynolds diagram, whereas weak points are given in terms of pressure losses. Heat transfer properties are also supported by detailed velocity fields measured within the channels by using micro Particle Image Velocimetry (μPIV). Moreover, the innovative choice to assemble the micro-channels in an adiabatic material is developed in view of an easy implementation of micro heat exchangers on existing applications.

2 Materials and methods

The experimental setup consists of a micro cell heated by a hot plate and fed by a syringe pump. The setup, sketched in Figure 1, is designed to carry out temperature measurements and micro Particle Image Velocimetry (μPIV) measurements to investigate the thermal aspects and the fluid dynamics of the different micro cell geometries tested in this work. The syringe Pump Landgraff LA-800 is provided with a 140 ml syringe and can be set at different flow rates in the range from 113 μl/hr to 12060 ml/hr. Distilled Water is used as the working fluid. The hot plate Stuart US-150 is used to maintain the system under a constant heat flux, while K-type thermocouples are used to measure the outlet water and the micro cell surface temperatures, as sketched in Figure 1. The micro cell is placed under a high-speed camera to acquire high resolution images of the region of interest. Both camera images and thermocouples data were collected and transferred to a PC with a frequency of one data per second for a total number of 1400 values for the thermocouples and 14000 images for the camera, setting a frame

rate of 10000 fps. To carry out µPIV measurements, the water is seeded by hollow glass spherical tracers with mean size equal to 15 µm and characterized by a Stokes time scale equal to $13.75 * 10^{-6}$ s. High resolution images are acquired with the high-speed camera Photron Mini AX100 starting from 4000 frames/s at full resolution of 1024x1024 pixels, up to 10000 frames/s at 768x528 pixels. Two consecutive frames are analyzed in order to determine the flow tracer displacements using cross-correlation algorithms with window offset and deformation (final sub-window size equal to 16*16 pixel). The flow field is investigated at velocities of 0.5 m/s (flow rate of 30 ml/min and Re = 500) and 1.5 m/s (flow rate of 90 ml/min and Re = 1500) with an error in flow rate measurement about ±0.05 ml/min.

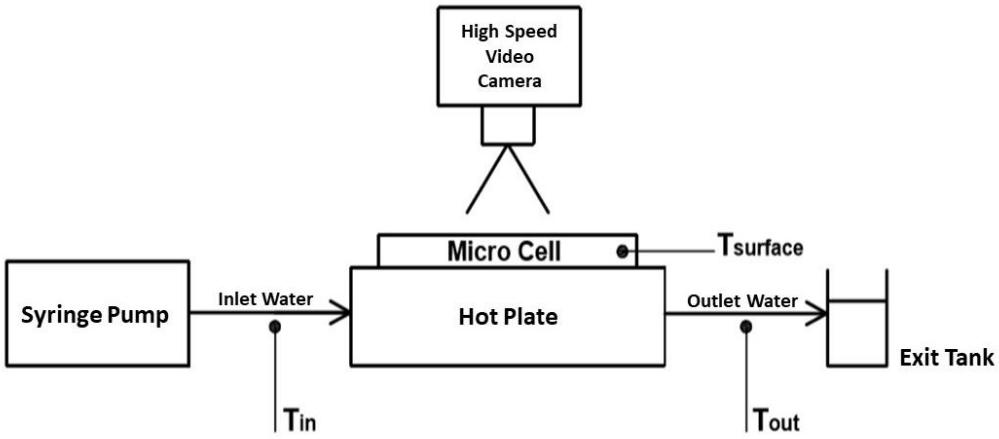

Figure 1: Sketch of the experimental setup

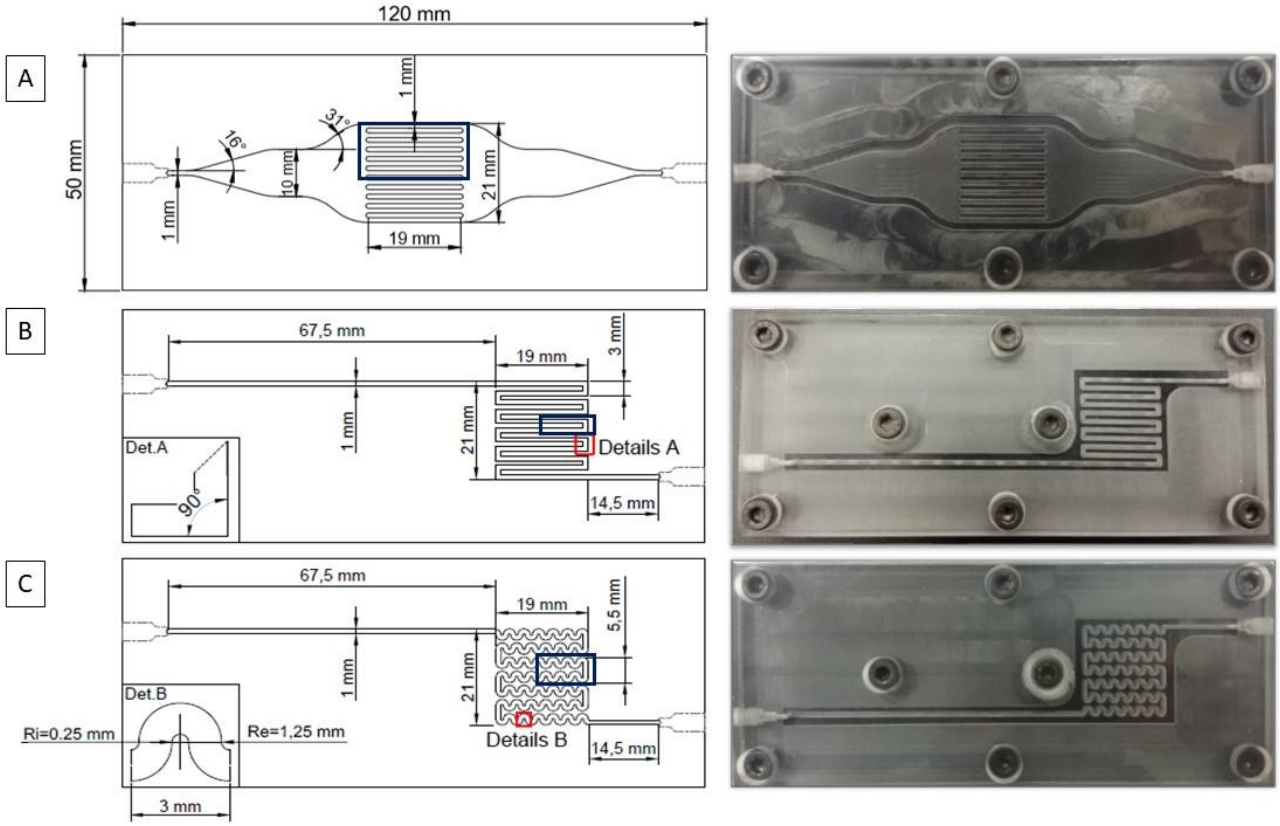

Figure 2: Technical scheme (left column) and picture (right column) of the top view of the micro-cells. A) straight parallel channels, B) standard serpentine, C) wavy serpentine

The thermal measurements have been performed in a range of velocities between 0.1 m/s (flow rate of 6 ml/min) to 4 m/s (flow rate of 240 ml/min), thus resulting in a minimum Reynolds number around 100 and a maximum Reynolds number around 4000, and setting up two constant temperature values of the hot source equal to 50 and 70 °C. The hot source is in direct contact with the micro cell bottom side (see Figure 1). Temperature data of the water at the outlet of the micro cell and the cooled surface are acquired by four thermocouples (K-type). One of the thermocouples is dived in the outlet water flow, while the other three are positioned inside the bottom side, in the middle of the heat exchange area and at a depth of 0.5 mm. The K-type thermocouples have a resolution of 0.1°C and an accuracy of ±1 °C. The micro devices with different geometries are composed of an aluminum bottom side and a plexiglas top side. The micro channel is milled on the adiabatic part of the micro cell to help cooling by micro heat exchangers application on existing industrial devices. Each U-element of the geometry has two horizontal sections with a length of 19 mm and a vertical section with a length of 3 mm. The Serpentine-B is a wavy serpentine channel with an heat exchange area of 354 mm^2 and an equivalent length equal to 354 mm. Each wavy element has an inner radius of 0.25 mm and an external radius of 1.25 mm. This configuration is also characterized by U-elements with two horizontal sections with a length of 19 mm and a vertical section with a length of 5.6 mm. Both the configurations present a test section of 19 mm x 21 mm and an inlet channel length of 67 mm to allow a complete development of the thermal and velocity fields.

3 Background and definitions

The diffusion of momentum in a fluid, associated with the development of the hydrodynamic boundary layer, and the diffusion of heat, associated with the development of the thermal boundary layer, are related phenomena, described by the Prandtl number (Massoud (2005)):

$$\mathrm{Pr} = \frac{\upsilon}{\alpha} = \frac{\mu \cdot c_p}{k} \tag{1}$$

where υ and μ are the cinematic and dynamic viscosity, respectively, c_p is the specific heat, α is the thermal diffusivity and k is the fluid thermal conductivity. The simultaneous development of both layers greatly influences the temperature profile and thus the heat transfer by convection,

$$\dot{q}_{Conv} = h \cdot (T_w - T_\infty), \qquad h = \frac{-k_{fluid} \cdot (\frac{\partial T}{\partial y})_{y=0}}{(T_w - T_\infty)} \tag{2}$$

where h is the convective heat transfer coefficient, T_∞ is the flow temperature, T_w is the average inner wall temperature and $(\frac{\partial T}{\partial y})_{y=0}$ denotes the temperature gradient along y axis. The mean Nusselt number accounts for the relative importance of convective to conductive heat transfer at the surface. In a heated micro channel under a constant heat flux condition it is generally obtained from the experimental data as (Lee et al. (2004), Massoud (2005), Morini et al. (2013)):

$$\overline{Nu} = \left(\frac{D_h}{k_{fluid}}\right) \times \frac{\dot{m} C_p (T_{b,out} - T_{b,in})}{A_s (T_w - T_b)} \tag{3}$$

where ṁ is the mass flow rate, C_p is the fluid specific heat and k_{fluid} is the fluid thermal conductivity, calculated at the fluid average bulk temperature, defined as the mean value between the bulk fluid temperature at the inlet and the outlet of the channel, D_h denotes the hydraulic diameter and A_s is the heated micro channel surface area. The main features of each geometry are reported in Table1. In addition, the dynamic effects due to the fluid flow are retained in the Reynolds number and in heat

transfer devices, the interactions among flow and thermal fields are usually reported in terms of Nusselt number as a function of Reynolds number, for a given Prandtl number (Massoud (2005) and Morini et al. (2013)). Following previous works, such as Mahmud et al. (2001) and Romano et al. (2014) , another indicator of the local contribution to mixing and heat exchange is given by the local rate of entropy production, assuming convective motions without internal heat generation. Since any non-equilibrium process is an irreversible process, due to the second law of thermodynamics, it is possible to define the entropy production, S, as a function of temperature and velocity gradients.

$$S = \frac{k}{T_0^2}\left[\left(\frac{\partial T}{\partial x}\right)^2 + \left(\frac{\partial T}{\partial y}\right)^2\right] + \frac{\mu}{T_0^2}\left[2\left\{\left(\frac{\partial u}{\partial x}\right)^2 + \left(\frac{\partial v}{\partial y}\right)^2\right\} + \left(\frac{\partial u}{\partial y} + \frac{\partial v}{\partial x}\right)^2\right] \quad (4)$$

where T_0 is the reference temperature of the system.

Channel Type	Area (mm^2)	Channel length L (mm)	D_h (mm)	Length ratio L_A/L	Diameter ratio D_{hA}/D_h
Straight Parallel Channels - (A)	947	101	2	1	1
Standard Serpentine - (B)	297	297	1	0.34	2
Wavy Serpentine - (C)	354	354	1	0.29	2

Table 1: Geometrical parameters of the three tested micro-cells

4 Thermal results

In this section, the heat exchange capability of the standard serpentine and the wavy serpentine micro cells are quantified and compared with the straight parallel channels in a range of Reynolds numbers 100<Re<4000, with a constant temperature value of the hot source set to 70 °C. To obtain the Nusselt number in each condition, the equilibrium temperature reached by the outlet water and the surface after thermal transients has been estimated. In both cases, the equilibrium temperature is analytically determined for each flow rate, on the base of a physical model applied simultaneously to all experimental data at different flow rates, by iterative least square interpolations. An example of the acquired trends towards the equilibrium temperature is presented in Figure 3 for the straight parallel channels configuration. All the experimental measurements are taken with a temperature gradient between inlet water and heated wall of about 50 °C, i.e. $T_{b,in} = 21°C$. In all measurements, initially the temperature decreases rapidly from values close to the hot source temperature (around 65°C for water) to a plateau after a thermal transient, whose duration is a function of the flow rate, i.e. of the Reynolds number. The increase of the flow rate also modifies the final temperatures reached by water and cooled surface. The results show that, as the flow rate increases, the amount of heat transferred to the water between the inlet and outlet is reduced, due to a lower travel time of the cooling fluid inside the device. Figure 4 shows the Nusselt number as a function of Re for the three micro-cells, with error bars and together with the classical correlations proposed by Sieder & Tate (1936) and Gnielinski (1995). In the inset the Nusselt values for 1000<Re<5000 are highlighted to better show the trend of the curves in the turbulent regime. Looking at Figure 4, it is immediately noticeable that both cells with serpentines (standard and wavy) show larger Nusselt numbers than those of the parallel channel configuration, for a given Reynolds number. Moreover, Nusselt number increases with Reynolds number with a power-law with exponent around 0.5 for all geometries, in agreement with theoretical predictions and Sieder-Tate empirical law (Sieder & Tate (1936)). Being Nusselt number a measure of heat flux due to convection, the impact of geometry and flow regime on convective motions is clearly shown in this plot. The serpentine with wavy channel attains the highest values of Nusselt number, suggesting that this geometry allows the most efficient heat transfer, only slightly lower values being obtained for the standard serpentine. On the other hand, the results for the parallel channel configuration show less

efficiency, the reasons for all these behaviors must be still detailed. Considering also the different flow regimes, it is possible to observe only a small change in slope when moving from laminar to turbulent regimes, not in agreement with Gnielinski suggestions (Gnielinski (1995)). Presumably, this is a consequence of using a non-classical channel shape, whereas the empirical laws are tuned for strictly linear circular section micro-channels. Therefore, it seems that the largest differences among the tested geometries are attained in laminar conditions, whereas they are less pronounced in the turbulent regime. This could be given to the fact that the serpentine configurations in comparison to parallel channels could promote flow acceleration and recirculation already in laminar conditions, and that these differences would be attenuated in fully established turbulence.

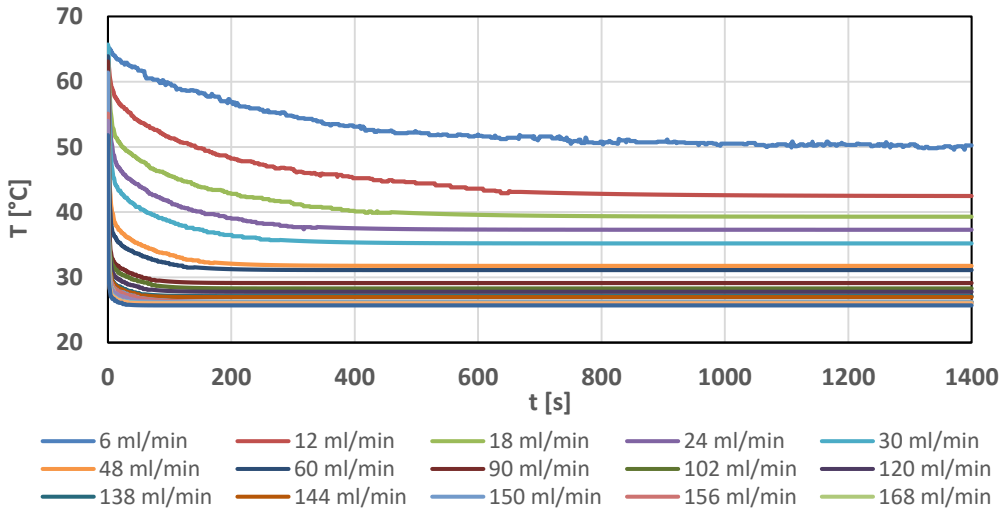

Figure 3: Water equilibrium temperatures as a function of time [s] and flow rate [ml/min] for the straight parallel channels micro cell at 70°C

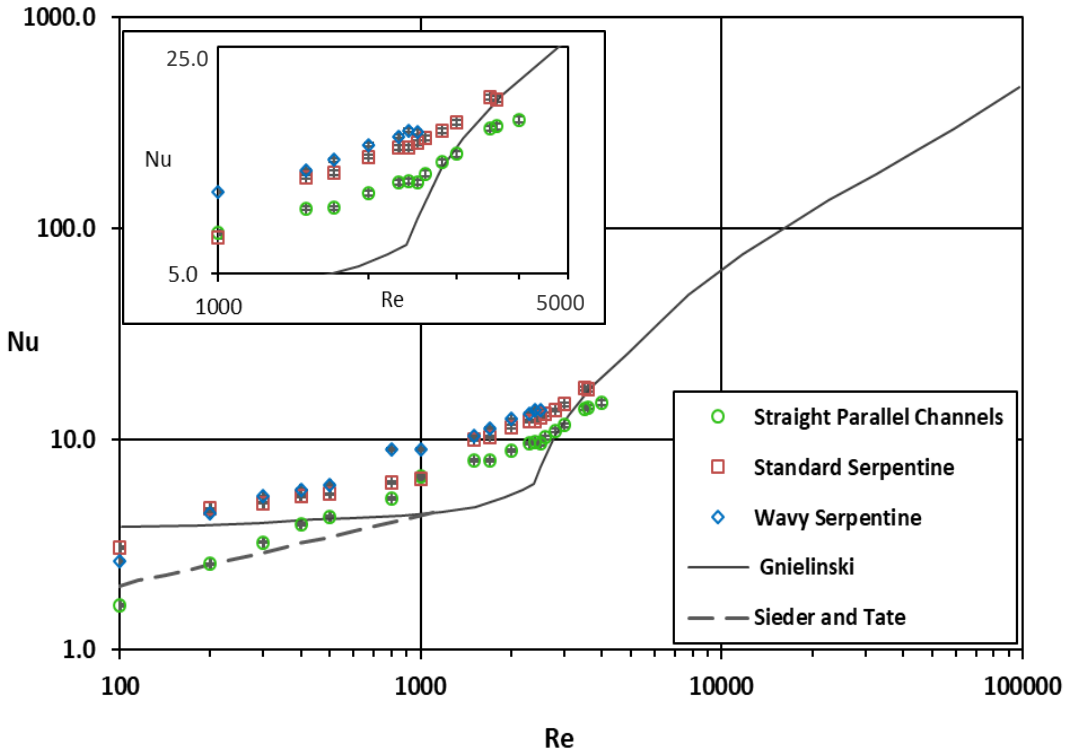

Figure 4: Comparison of the Average Nusselt numbers as a function of the Reynolds number obtained for the three tested micro-cells with the correlations proposed by Sieder & Tate (1936) and Gnielinski (1995)

5 µPIV Results

In this section, Particle Image Velocimetry is employed to characterized the velocity field of the three micro-cells, in order to make a link with results highlighted by the thermal measurements. Specifically, the attention will be focused on local fluid recirculation and acceleration as related to the specific geometry and to the different flow rates. In Figure 5 the velocity vectors map of the three micro-cells are compared at a flow rate of 30 ml/min, for the parallel channel configuration being represented both inner and outer sections. For the serpentine configurations, images were acquired far from the inlet channel in order to have a completely developed flow field (the acquisition areas are delimited in blue in Figure 2). The results reported for the parallel channel configuration, Figure 5a, show a very uniform inlet and outlet flow, with only a few relevant modifications. These are located at the inlet of each channel, giving rise to local accelerations without any relevant separation, and in the form of separated recirculating regions at the outlet crossings of different channels. On the other hand, for the standard serpentine cell, Figure 5b, at each 90° bend, a strong separation is observed, with both local acceleration and three-dimensional motion (as shown also in Liou et al. (2018)). This could highly increase the local heat transfer, especially as a consequence of the local accelerations and of the relatively large residual channel size. A similar condition is observed also for the wavy serpentine cell, Figure 5c, showing periodic large flow recirculation and reduced channel size, even if with large local accelerations. Again, this contributes to a local increase of heat transfer, but also to a simultaneous decrease due to the reduced available channel size. These results are in agreement with thermal measurements, showing that the main reason for the increasing Nusselt number for serpentine cells is dependent on local high intensity accelerations. This situation takes place even at relatively small Reynolds numbers, when fully turbulence effects are still far to be established. In order to better appreciate the differences in the fluid flows of the three cells, color maps of the average normalized velocity magnitude, vorticity fields and entropy, as defined in section 3, for a flow rate of 30 ml/min are reported in Figure 6, Figure 7 and Figure 8, respectively.

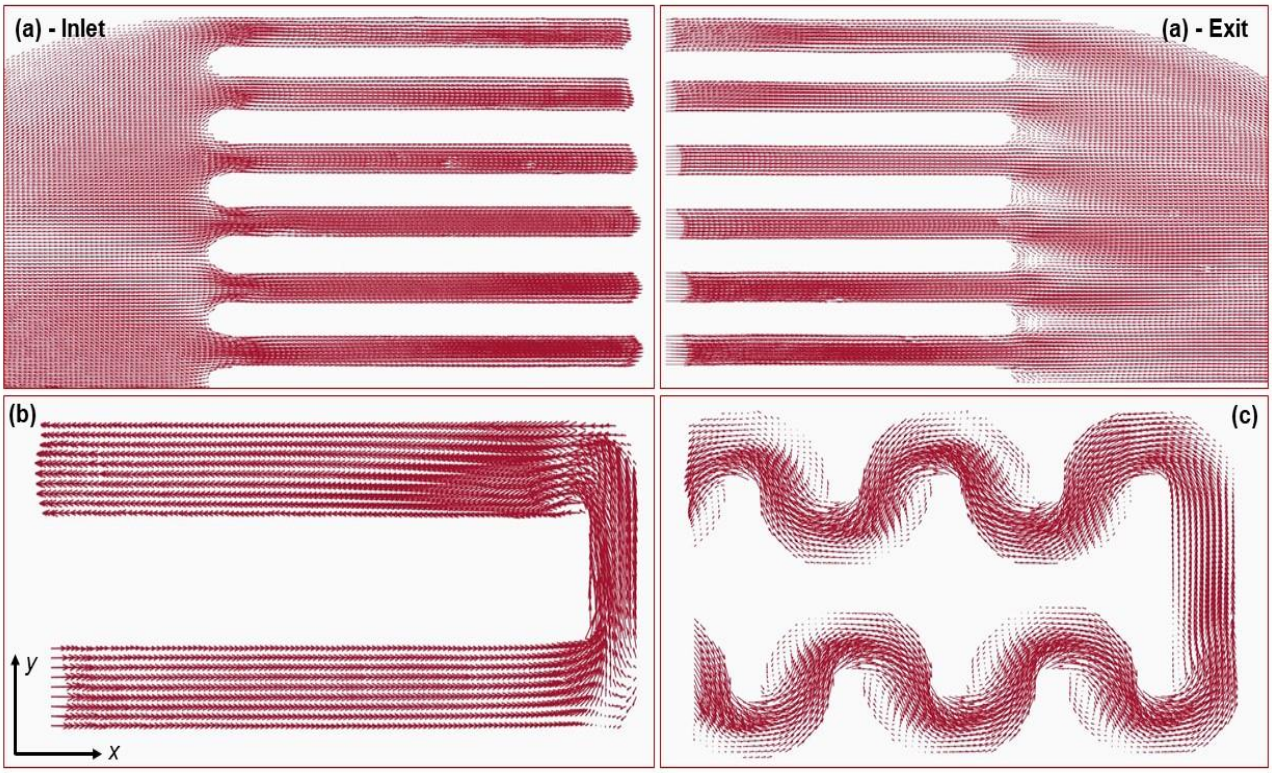

Figure 5: Mean velocity vectors fields at 30 ml/min. (a) straight parallel channels, (b) standard serpentine, (c) wavy serpentine

The yellow regions in Figure 6 represent quite high local velocities attained in the two serpentine geometries (note the change in scale range), with related low velocity regions (accordingly to Liou et al. (2018)). Indeed, in these high velocity sections, where the magnitude of the normalized velocity is larger than one, the average velocity is highly exceeded. In Figure 6a, for the parallel channel geometry, it is also shown how the total flow rate is subdivided non-uniformly into the single channels. Actually, the large part of the flow, i.e. more than 60% of the total flow arte, crosses the central five channels (only one half of the flow field is shown). In Figure 7 we can observe a growth in the level of vorticity from geometry (a), where it is limited to boundary layers, to geometry (b), where the vorticity is given by boundary layers in the straight sections and by recirculation regions in the bending sections and to geometry (c), which shows vorticity of opposite sign. Therefore, results in Figure 6 and Figure 7 show that the local fluid mechanics motivation for improved global heat transfer performances in serpentine rather than linear configurations possibly derives from the simultaneous presence of recirculation and acceleration regions. As reported in section 3 of this paper and in Hashiehbaf & Romano (2014), the local entropy production rate gives a measure of mixing and heat transfer capability, so far being here used to quantify the previous statement. To this aim, mean entropy production rate is shown in Figure 8 for all configurations, made non-dimensional by dividing it by bulk velocity, channel diameter and hot source temperature taken as reference temperature. At a first sight, it is clear that such a production basically vanishes all over the field for the parallel channel configuration, except for boundary layers and the outlet crossing of the channels. On the other hand, the highest entropy is achieved in the standard serpentine cell, being related to the local flow acceleration and not to the recirculation, as confirmed by the comparison with Figure 5 and Figure 6. This is established also for the wavy serpentine configuration, where the highest entropy values, slightly lower than the previous case, are related to the local increment of velocity. Therefore, the recirculation regions do not contribute to mixing and heat transfer increment, rather only to pressure loss increments.

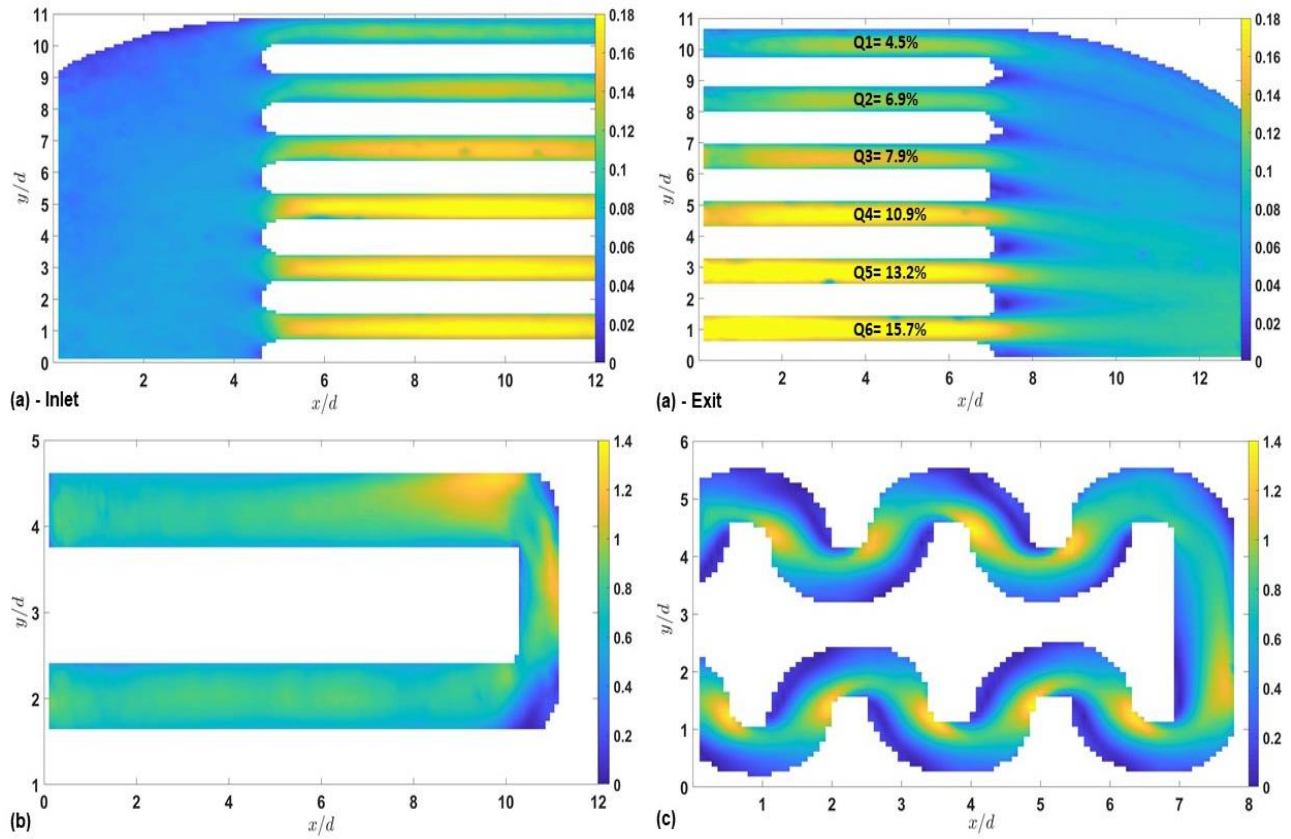

Figure 6: Mean velocity magnitude color maps at 30 ml/min. (a) straight parallel channels, (b) standard serpentine, (c) wavy serpentine

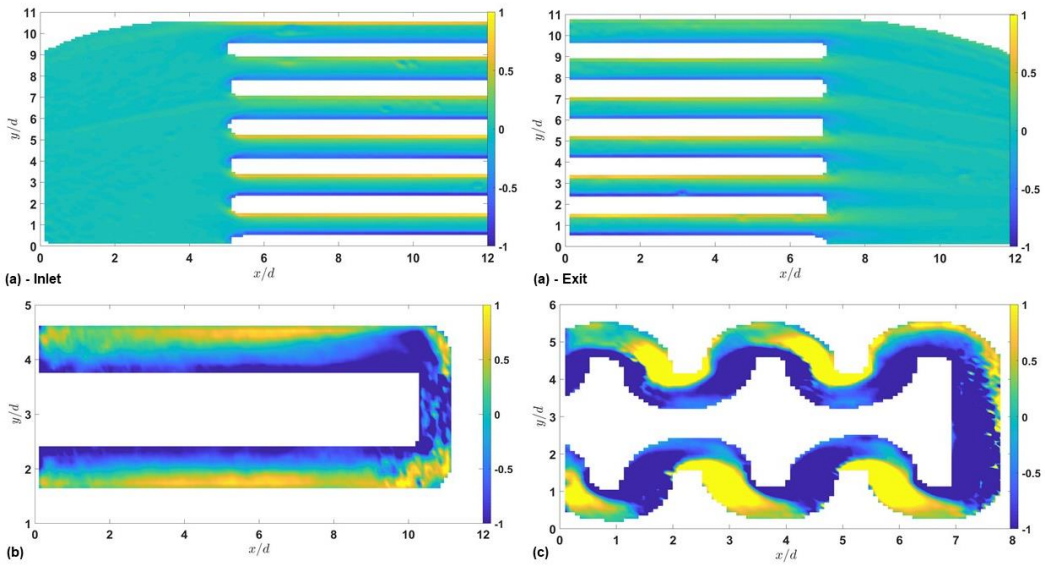

Figure 7: Mean vorticity color maps at 30 ml/min. (a) straight parallel channels, (b) standard serpentine, (c) wavy serpentine

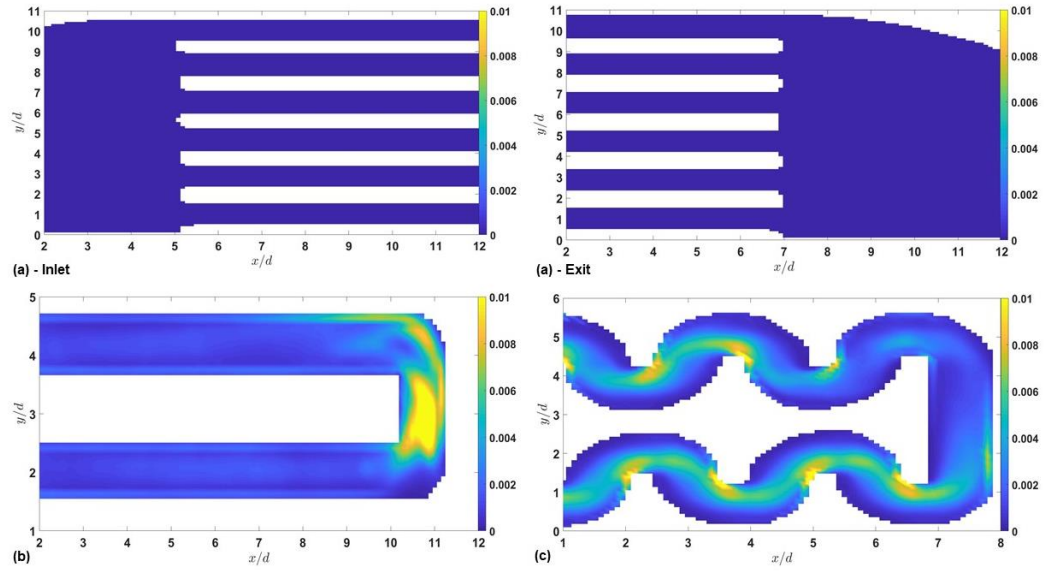

Figure 8: Mean entropy fields at 30 ml/min. (a) straight parallel channels, (b) standard serpentine, (c) wavy serpentine

6 Acknowledgment

The authors would like to thank Dr. Camilla Cecchini and the graduate student Alireza Hassani Sorkhani for the collaboration in experimental tests.

References

Al-Neama AF, Kapur N, Summers J and Thompson HM (2017) An experimental and numerical investigation of the use of liquid flow in serpentine microchannels for microelectronics cooling. *Applied Thermal Engineering* 116:709-723

Asako Y, Nakamura H and Faghri M (1988) Heat transfer and pressure drop characteristics in a corrugated duct with rounded corners. *International Journal of Heat and Mass Transfer* 31:1237-1245

Eshani M, Gao Y, Gay ES and Emadi A (2005) *Modern Electric, Hybrid Electric, and Fuel Cell Vehicles*. Chapter Electric Vehicles, page 98. CRC Press. 3rd edition

Fehle R, Klas J and Mayinger F (1995) Investigation of local heat transfer in compact heat exchangers by holographic interferometry. *Experimental Thermal and Fluid Science* 10:181-191

Gaiser G and Kottke V (1989) Flow phenomena and local heat and mass transfer in corrugated passages. *Chemical and Engineering Technology* 12:400-405

Gnielinski V (1995) Ein Neues Berechnungsverfahren fur die Warmeubertragung im Ubergangsbereich zwischen Laminaren und Turbulenter Rohstromung. *Forschung im Ingenieurwesen* 61*:*240-248

Hashiehbafa A, Romano GP (2014) An experimental investigation on mixing enhancements in non-circular sharp-edged nozzles using the entropy production concept. *Journal of Turbulence* 15*:*411-428

Herman CV, Mayinger F and Sekulic DP (1991) Experimental verification of oscillatory phenomena in heat transfer in a communicating channels geometry. *Experimental Heat Transfer, Fluid Mechanics and Thermodynamics* 1:904-911

Kandlikar SG (2012) History, Advances, and Challenges in Liquid Flow and Flow Boiling Heat Transfer in Microchannels: A Critical Review. *Journal of Heat Transfer* 134:034001–034015

Kandlikar SG, Colin S, Peles Y, Garimella S, Pease RF, Brandner JJ and Tuckerman DB (2013) Heat Transfer in Microchannels 2012 Status and Research Needs. *Journal of Heat Transfer* 135:091001

Lee P, Garimella SV and Liu D (2004) Investigation of heat transfer in rectangular microchannels. *International Journal of Heat and Mass Transfer* 48:1688-1704

Lin L, Zhao J, Lu G, Wang XD, Yan WM (2017) Heat transfer enhancement in microchannel heat sink by wavy channel with changing wave length/amplitude. *International Journal of Thermal Sciences* 118:423-434

Liou TM, Wang CS and Wang H (2018) Nusselt number and friction factor correlations for laminar flow in parallelogram serpentine micro heat exchangers. *Applied Thermal Engineering* 143:871-882

Mahmud S and Fraser RA (2001) The second law analysis in fundamental convective heat transfer problems. *International Journal of Thermal Sciences* 42:177-186

Massoud M (2005) *Engineering Thermofluids-Thermodynamics, Fluid Mechanics and Heat Transfer*. Chapter Heat Transfer: Forced Convection, page 520. Springer. 1rd edition

Morini GL and Yang Y (2013) Guidelines for the Determination of Single-Phase Forced Convection Coefficients in Microchannels. *Journal of Heat Transfer* 135:101004

Sieder EN and Tate GE (1936) Heat Transfer and Pressure Drop of Liquids in Tubes. *Ind. Eng. Chem.* 28:1429-1435

Sui Y, Lee PS and Teo CJ (2011) An experimental study of flow friction and heat transfer in wavy microchannels with rectangular cross section. *International Journal of Thermal Sciences* 50:2473-2482